# Supporting Information

# A new salicylaldehyde-based azo dye and its two lanthanide(III) complexes displaying slow magnetic relaxation

Jian-Qiang He,[a] Shang-Fang Xie,[a] Bi-Lin Lai,[a] Meng Yang,[a] Wen-Bin Chen,*[a] Yi-Quan Zhang*[b] and Wen Dong*[a]

a. Guangzhou Key Laboratory for Environmentally Functional Materials and Technology, School of Chemistry and Chemical Engineering, Guangzhou University, Guangzhou 510006, P. R. China. E-mail: 772694131@qq.com; dw320@aliyun.com.

b. Jiangsu Key Laboratory for NSLSCS, School of Physical Science and Technology, Nanjing Normal University, Nanjing 210023, P. R. China. E-mail: zhangyiquan@njnu.edu.cn.

Table S1 SHAPE analysis for **1** and **2**.

| Complex | Ln | SAPR-8 | TDD-8 | JBTPR-8 | BTPR-8 |
|---|---|---|---|---|---|
| **1** | **Dy1** | **0.513** | 1.822 | 1.871 | 1.623 |
| | **Dy2** | **0.679** | 1.244 | 1.927 | 1.552 |
| **2** | **Tb1** | **0.516** | 1.702 | 1.923 | 1.673 |
| | **Tb2** | **0.693** | 1.252 | 1.963 | 1.677 |

SAPR-8 = square antiprism; TDD-8 = triangular dodecahedron; JBTPR-8 = Biaugmented trigonal prism J50; BTPR-8 = Biaugmented trigonal prism; JSD-8 = Snub diphenoid J84.

Table S2. The bond lengths [Å] and angles [°] for complex **1** and **2**.

| | | | |
|---|---|---|---|
| Dy(1)-O(1) | 2.373(5) | Tb(1)-O(1) | 2.384(8) |
| Dy(1)-O(2) | 2.350(5) | Tb(1)-O(2) | 2.351(8) |
| Dy(1)-O(3) | 2.400(5) | Tb(1)-O(3) | 2.415(8) |
| Dy(1)-O(4) | 2.301(5) | Tb(1)-O(4) | 2.313(8) |
| Dy(1)-O(6) | 2.453(6) | Tb(1)-O(6) | 2.472(7) |
| Dy(1)-O(7) | 2.283(5) | Tb(1)-O(7) | 2.287(7) |
| Dy(1)-O(9) | 2.388(5) | Tb(1)-O(9) | 2.386(7) |
| Dy(1)-O(10) | 2.284(5) | Tb(1)-O(10) | 2.290(8) |
| Dy(2)-O(12) | 2.342(5) | Tb(2)-O(12) | 2.349(8) |
| Dy(2)-O(13) | 2.475(5) | Tb(2)-O(13) | 2.481(8) |

| | | | |
|---|---|---|---|
| Dy(2)-O(14) | 2.256(5) | Tb(2)-O(14) | 2.278(8) |
| Dy(2)-O(16) | 2.392(5) | Tb(2)-O(16) | 2.406(8) |
| Dy(2)-O(17) | 2.395(6) | Tb(2)-O(17) | 2.418(8) |
| Dy(2)-O(18) | 2.298(5) | Tb(2)-O(18) | 2.315(8) |
| Dy(2)-O(20) | 2.383(5) | Tb(2)-O(20) | 2.394(8) |
| Dy(2)-O(21) | 2.325(5) | Tb(2)-O(21) | 2.333(7) |
| O(1)-Dy(1)-O(3) | 72.79(19) | O(1)-Tb(1)-O(3) | 72.6(3) |
| O(1)-Dy(1)-O(6) | 121.42(19) | O(1)-Tb(1)-O(6) | 121.9(3) |
| O(1)-Dy(1)-O(9) | 75.31(18) | O(1)-Tb(1)-O(9) | 75.4(3) |
| O(2)-Dy(1)-O(1) | 70.18(18) | O(2)-Tb(1)-O(1) | 70.4(3) |
| O(2)-Dy(1)-O(3) | 86.41(19) | O(2)-Tb(1)-O(3) | 85.9(3) |
| O(2)-Dy(1)-O(6) | 73.39(18) | O(2)-Tb(1)-O(6) | 74.1(3) |
| O(2)-Dy(1)-O(9) | 143.50(18) | O(2)-Tb(1)-O(9) | 143.7(3) |
| O(3)-Dy(1)-O(6) | 147.10(17) | O(3)-Tb(1)-O(6) | 147.2(2) |
| O(4)-Dy(1)-O(1) | 133.21(18) | O(4)-Tb(1)-O(1) | 132.7(3) |
| O(4)-Dy(1)-O(2) | 78.00(19) | O(4)-Tb(1)-O(2) | 77.4(3) |
| O(4)-Dy(1)-O(3) | 71.82(18) | O(4)-Tb(1)-O(3) | 71.4(3) |
| O(4)-Dy(1)-O(6) | 78.63(18) | O(4)-Tb(1)-O(6) | 79.0(3) |
| O(4)-Dy(1)-O(9) | 120.18(19) | O(4)-Tb(1)-O(9) | 120.2(3) |
| O(7)-Dy(1)-O(1) | 75.06(18) | O(7)-Tb(1)-O(1) | 75.8(2) |
| O(7)-Dy(1)-O(2) | 104.71(19) | O(7)-Tb(1)-O(2) | 105.5(3) |
| O(7)-Dy(1)-O(3) | 139.80(18) | O(7)-Tb(1)-O(3) | 140.2(2) |
| O(7)-Dy(1)-O(4) | 147.86(18) | O(7)-Tb(1)-O(4) | 147.8(3) |
| O(7)-Dy(1)-O(6) | 71.84(17) | O(7)-Tb(1)-O(6) | 71.4(2) |
| O(7)-Dy(1)-O(9) | 76.88(18) | O(7)-Tb(1)-O(9) | 76.8(3) |
| O(7)-Dy(1)-O(10) | 80.47(18) | O(7)-Tb(1)-O(10) | 80.2(3) |
| O(9)-Dy(1)-O(3) | 72.15(18) | O(9)-Tb(1)-O(3) | 72.5(3) |
| O(9)-Dy(1)-O(6) | 137.62(17) | O(9)-Tb(1)-O(6) | 137.0(2) |
| O(10)-Dy(1)-O(1) | 143.38(18) | O(10)-Tb(1)-O(1) | 143.5(3) |
| O(10)-Dy(1)-O(2) | 143.62(18) | O(10)-Tb(1)-O(2) | 143.7(3) |
| O(10)-Dy(1)-O(3) | 113.13(19) | O(10)-Tb(1)-O(3) | 112.9(3) |
| O(10)-Dy(1)-O(4) | 79.61(18) | O(10)-Tb(1)-O(4) | 79.8(3) |
| O(10)-Dy(1)-O(6) | 74.34(18) | O(10)-Tb(1)-O(6) | 74.1(3) |
| O(10)-Dy(1)-O(9) | 72.87(18) | O(10)-Tb(1)-O(9) | 72.6(3) |
| O(12)-Dy(2)-O(13) | 73.88(18) | O(12)-Tb(2)-O(13) | 74.6(2) |
| O(12)-Dy(2)-O(16) | 73.37(18) | O(12)-Tb(2)-O(16) | 73.7(3) |
| O(12)-Dy(2)-O(17) | 83.91(18) | O(12)-Tb(2)-O(17) | 84.2(3) |
| O(12)-Dy(2)-O(20) | 145.01(19) | O(12)-Tb(2)-O(20) | 145.0(2) |
| O(14)-Dy(2)-O(12) | 106.24(19) | O(14)-Tb(2)-O(12) | 106.5(3) |
| O(14)-Dy(2)-O(13) | 70.89(18) | O(14)-Tb(2)-O(13) | 70.1(2) |
| O(14)-Dy(2)-O(16) | 72.37(18) | O(14)-Tb(2)-O(16) | 72.2(2) |
| O(14)-Dy(2)-O(17) | 138.83(18) | O(14)-Tb(2)-O(17) | 139.1(3) |
| O(14)-Dy(2)-O(18) | 147.40(19) | O(14)-Tb(2)-O(18) | 147.4(3) |

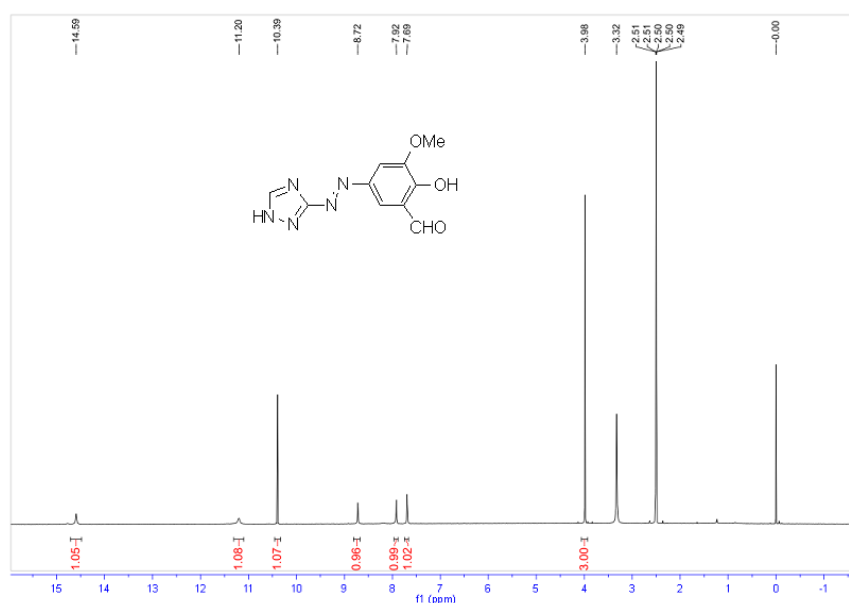| | | | |
|---|---|---|---|
| O(14)-Dy(2)-O(20) | 78.88(19) | O(14)-Tb(2)-O(20) | 78.5(3) |
| O(14)-Dy(2)-O(21) | 80.01(18) | O(14)-Tb(2)-O(21) | 79.9(2) |
| O(16)-Dy(2)-O(13) | 120.27(18) | O(16)-Tb(2)-O(13) | 120.1(3) |
| O(16)-Dy(2)-O(17) | 72.82(19) | O(16)-Tb(2)-O(17) | 73.5(3) |
| O(17)-Dy(2)-O(13) | 148.06(16) | O(17)-Tb(2)-O(13) | 148.9(3) |
| O(18)-Dy(2)-O(12) | 79.79(19) | O(18)-Tb(2)-O(12) | 79.9(3) |
| O(18)-Dy(2)-O(13) | 80.63(18) | O(18)-Tb(2)-O(13) | 81.5(3) |
| O(18)-Dy(2)-O(16) | 138.17(18) | O(18)-Tb(2)-O(16) | 138.5(3) |
| O(18)-Dy(2)-O(17) | 72.95(19) | O(18)-Tb(2)-O(17) | 72.5(3) |
| O(18)-Dy(2)-O(20) | 114.85(19) | O(18)-Tb(2)-O(20) | 114.9(3) |
| O(18)-Dy(2)-O(21) | 76.75(18) | O(18)-Tb(2)-O(21) | 76.6(2) |
| O(20)-Dy(2)-O(13) | 137.50(17) | O(20)-Tb(2)-O(13) | 136.5(2) |
| O(20)-Dy(2)-O(16) | 75.59(18) | O(20)-Tb(2)-O(16) | 75.2(3) |
| O(20)-Dy(2)-O(17) | 71.75(18) | O(20)-Tb(2)-O(17) | 71.9(3) |
| O(21)-Dy(2)-O(12) | 142.01(18) | O(21)-Tb(2)-O(12) | 141.9(2) |
| O(21)-Dy(2)-O(13) | 73.14(17) | O(21)-Tb(2)-O(13) | 72.6(3) |
| O(21)-Dy(2)-O(16) | 141.23(17) | O(21)-Tb(2)-O(16) | 141.0(2) |
| O(21)-Dy(2)-O(17) | 116.43(18) | O(21)-Tb(2)-O(17) | 116.0(3) |
| O(21)-Dy(2)-O(20) | 72.75(18) | O(21)-Tb(2)-O(20) | 72.9(2) |



Fig. S1 Schematic illustration for $^1$H NMR peaks of H$_2$TMSA in DMSO-d$^6$.
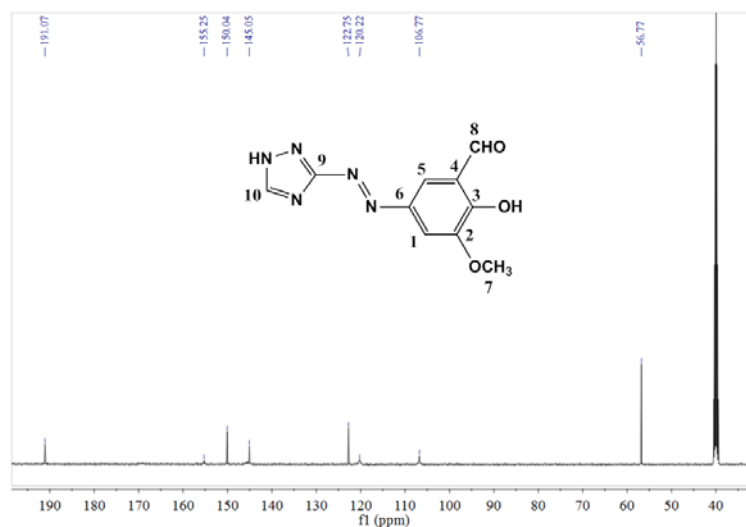
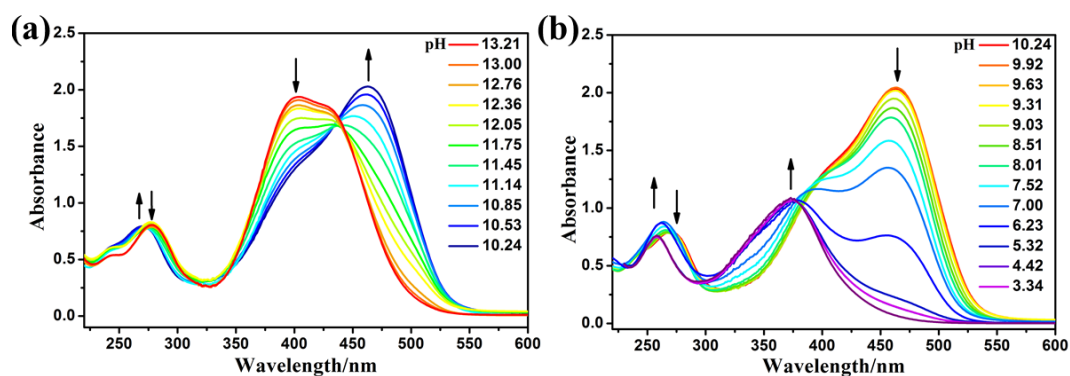Fig. S2 Schematic illustration for $^{13}C$ NMR peaks of $H_2TMSA$ in DMSO-$d^6$.



Fig. S3 Absorbance spectra of the TMSA in ethanol, after adjusted the pH value to 13.21, and recovered the pH value by the dilute solution of HCl (c = 1 mol L$^{-1}$). pH: 13.21-10.24 (a);10.24-3.34 (b). Arrows indicate changes in UV-vis absorption.
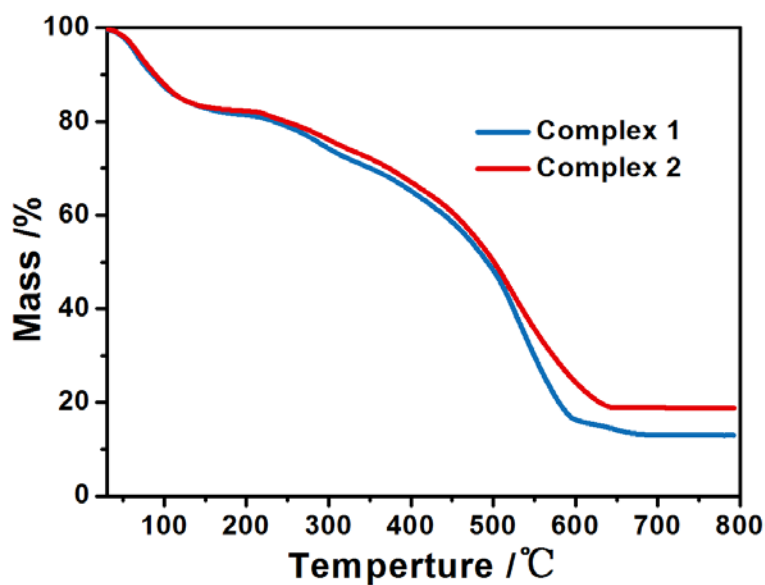


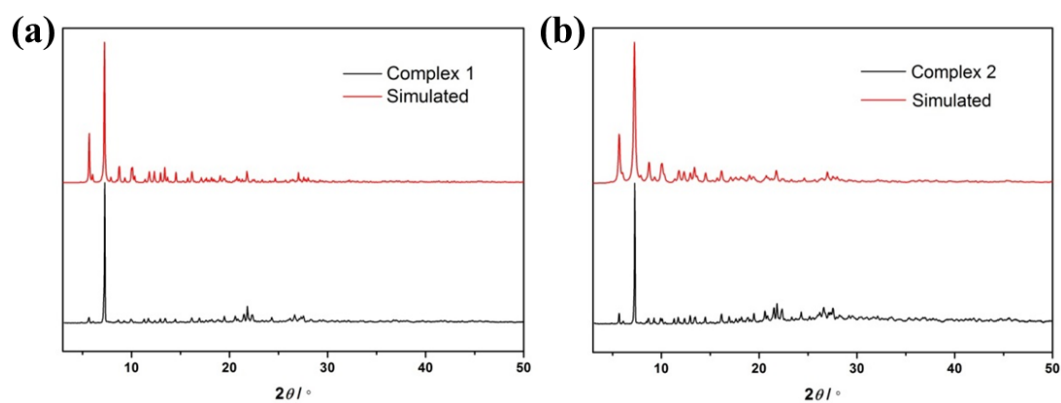Fig. S4 Thermal gravimetric analyses (TGA) curves for complex **1** and **2**.

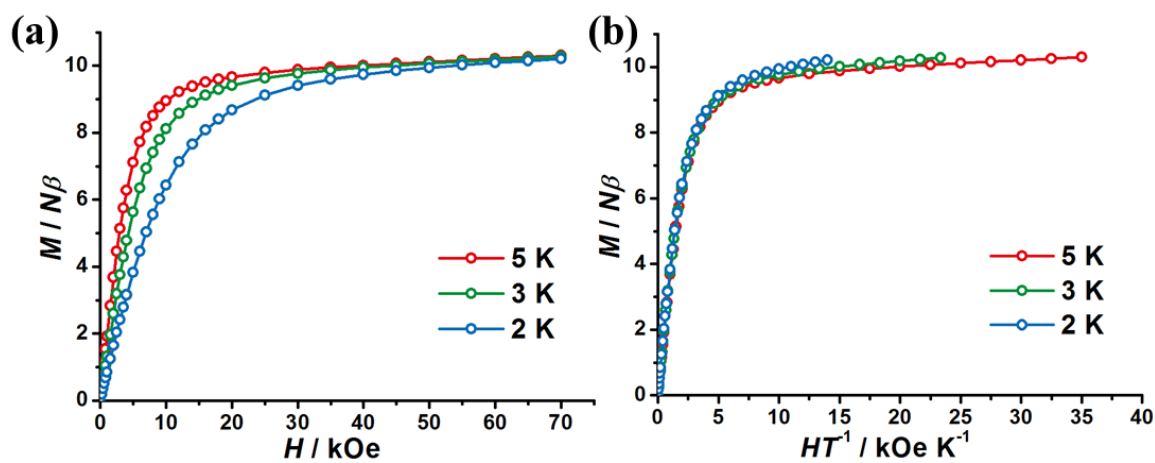Fig. S5 Powder X-ray diffraction (PXRD) patterns for complexes **1** and **2**.



Fig. S6 Plots of *M–H* (a) and *M–H/T* (b) for **1** at 2, 3 and 5 K. The solid lines are guides to the eyes.
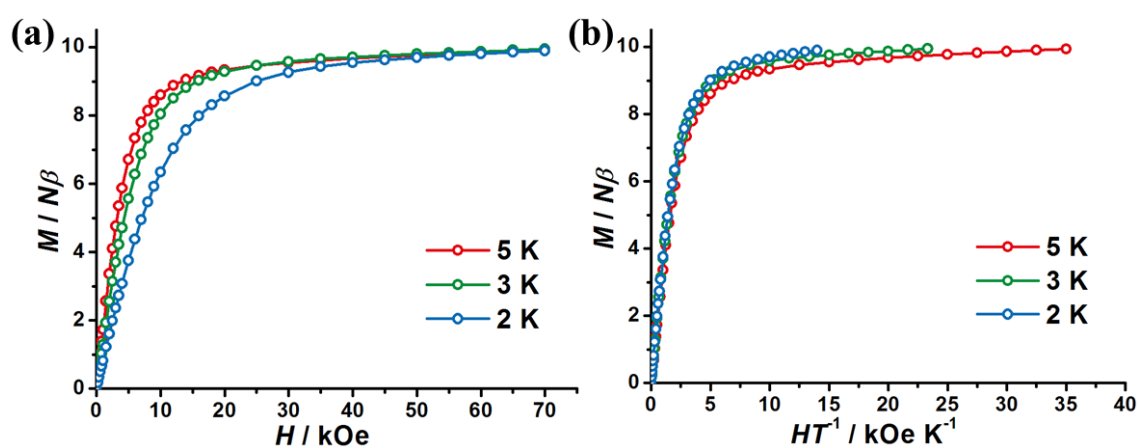


Fig. S7 Plots of *M–H* (a) and *M–H/T* (b) for **2** at 2, 3 and 5 K. The solid lines are guides to the eyes.
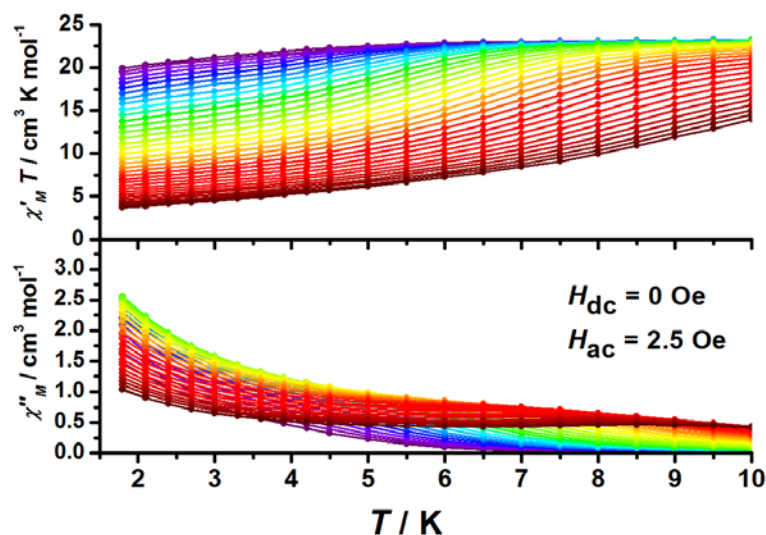
Fig. S8 Temperature dependence of the in-phase ($\chi_M'T$) and out-of-phase ($\chi_M''$) products at a zero field for **1**, with ac frequencies of 1−1000 Hz. The solid lines are guides to the eyes.

Table S3 Relaxation fitting parameters from Least-Squares Fitting of χ(ω) data for **1** at zero dc field.

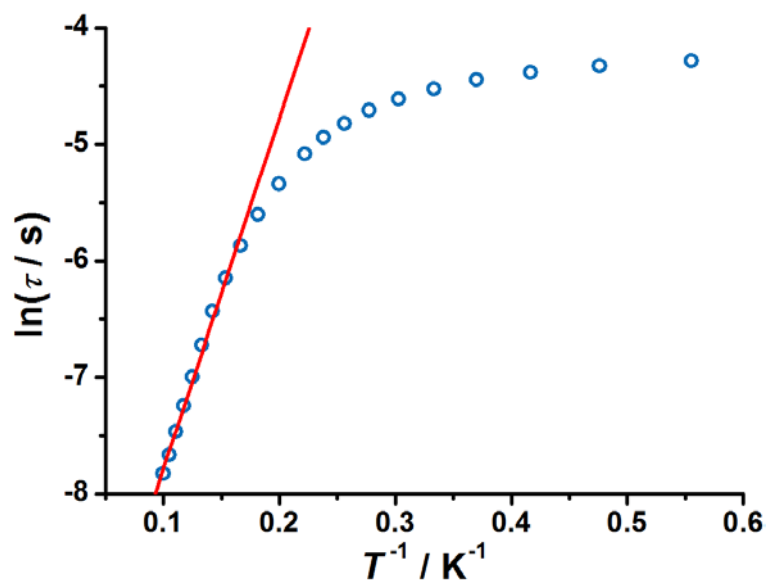| $T$ / K | $\tau$ | $\tau$ | $\alpha$ | $\alpha$ | $\chi_0$ | $\chi_0$ | $\chi_\infty$ | $\chi_\infty$ |
|---|---|---|---|---|---|---|---|---|
| | Value | Standard Error | Value | Standard Error | Value | Standard Error | Value | Standard Error |
| 10 | 4.00E-04 | 1.27E-05 | 0.26429 | 0.00893 | 2.34481 | 0.00377 | 0.98921 | 0.02017 |
| 9.5 | 4.68E-04 | 1.24E-05 | 0.25292 | 0.00818 | 2.46689 | 0.00404 | 0.97029 | 0.01882 |
| 9 | 5.72E-04 | 1.28E-05 | 0.24297 | 0.0076 | 2.6011 | 0.00441 | 0.96512 | 0.01738 |
| 8.5 | 7.15E-04 | 1.50E-05 | 0.23995 | 0.00772 | 2.75504 | 0.00534 | 0.95955 | 0.01769 |
| 8 | 9.17E-04 | 1.93E-05 | 0.24238 | 0.00816 | 2.92856 | 0.00675 | 0.95919 | 0.01877 |
| 7.5 | 0.0012 | 2.57E-05 | 0.25335 | 0.00854 | 3.12831 | 0.00852 | 0.96305 | 0.01989 |
| 7 | 0.0016 | 3.60E-05 | 0.27184 | 0.00902 | 3.3622 | 0.01098 | 0.97197 | 0.02157 |
| 6.5 | 0.00214 | 5.22E-05 | 0.29915 | 0.00963 | 3.6388 | 0.01455 | 0.97578 | 0.0242 |
| 6 | 0.00282 | 7.44E-05 | 0.33352 | 0.00996 | 3.97188 | 0.01911 | 0.96902 | 0.02706 |
| 5.5 | 0.00368 | 1.01E-04 | 0.36975 | 0.00987 | 4.36754 | 0.0244 | 0.94845 | 0.02953 |
| 5 | 0.00479 | 1.29E-04 | 0.40305 | 0.00914 | 4.84987 | 0.02949 | 0.92587 | 0.03039 |
| 4.5 | 0.0062 | 1.60E-04 | 0.42997 | 0.00822 | 5.43547 | 0.0345 | 0.91847 | 0.03029 |
| 4.2 | 0.00714 | 1.79E-04 | 0.44451 | 0.00768 | 5.85134 | 0.03767 | 0.91714 | 0.03029 |
| 3.9 | 0.00805 | 2.02E-04 | 0.45569 | 0.00734 | 6.31367 | 0.04169 | 0.92218 | 0.03108 |
| 3.6 | 0.00902 | 2.28E-04 | 0.46625 | 0.00708 | 6.87481 | 0.04684 | 0.92678 | 0.0325 |
| 3.3 | 0.00993 | 2.54E-04 | 0.47396 | 0.00691 | 7.50593 | 0.05271 | 0.94188 | 0.03443 |
| 3 | 0.01081 | 2.81E-04 | 0.47989 | 0.00678 | 8.2596 | 0.05968 | 0.9662 | 0.03696 |
| 2.7 | 0.01171 | 3.15E-04 | 0.48811 | 0.00673 | 9.18864 | 0.06943 | 0.98497 | 0.04089 |
| 2.4 | 0.01251 | 3.43E-04 | 0.49526 | 0.00661 | 10.34123 | 0.08025 | 1.0136 | 0.04537 |
| 2.1 | 0.01322 | 3.67E-04 | 0.5023 | 0.00646 | 11.75593 | 0.09271 | 1.05092 | 0.05065 |
| 1.8 | 0.01379 | 3.94E-04 | 0.50876 | 0.00643 | 13.54754 | 0.11001 | 1.10895 | 0.05858 |

Fig. S9 The plots of $\ln(\tau)$ vs. $T^{-1}$ for **1** under zero dc fields. The red line represents fit the data in the high temperature region with an Arrhenius law, resulting in an energy barrier $U_{\text{eff}}$ = 20.9(6) K, pre-exponential factor $\tau_0 = 2.0 \times 10^{-6}$ s.

Table S4 Selected Dy complexes with square antiprism geometry.

| Complexes | $U_{\text{eff}}$ / cm$^{-1}$ ($H_{\text{dc}}$ / Oe) | Ref |
|---|---|---|
| [Dy$_2$(acac)$_6$(bpe)(MeOH)$_2$]·bpe·2MeOH | 71.7 cm$^{-1}$ (1500 Oe) | Inorg. Chem. 2017, 56, 8829−8836.[1] |
| [Dy(acac)$_3$(bpe)]$_n$ | 33.7 cm$^{-1}$ (800 Oe) | |
| [(dtc)$_3$Dy(phen)] | 13.9 cm$^{-1}$ (400 Oe) | Dalton Trans., 2016, 45, 8149–8153.[2] |
| [(dbm)$_2$Dy(dtc)(phen)] | 27.8 cm$^{-1}$ (0 Oe)/31.2 cm$^{-1}$(1000 Oe) | |
| [Dy(acac)$_3$(H$_2$O)$_2$] | 45.9 cm$^{-1}$ (0 Oe) | Angew. Chem. Int. Ed. 2010, 49, 7448 – 7451.[3] |
| [hqH$_2$][Dy$_2$(hq)$_4$(NO$_3$)$_3$]·MeOH | 40.9 cm$^{-1}$ (1000 Oe) | Nat. Commun., 2014, 5, 5243.[4] |
| [TBA][Pc$_2$Dy] | 27.8 cm$^{-1}$ (0 Oe) | J. Am. Chem. Soc., 2003, 125, 8694-8695.[5] |
| [Dy(HATSA)(OAc)(H$_2$O)$_2$]·4H$_2$O | 2.4 cm$^{-1}$ (0 Oe)/25.5 cm$^{-1}$(1000 Oe) | Inorg. Chim. Acta, 2018, 469, 38-43.[6] |
| {[Dy(HTMSA)$_3$(H$_2$O)$_2$][Dy(HTMSA)$_3$(DMF)(H$_2$O)]}·15H$_2$O | 20.9 cm$^{-1}$ (0 Oe) | **This work** |

acac=acetylacetone; bpe= 1,2-bis(4-pyridyl)ethylene; dtc = diethyldithiocarbamate; dbm= dibenzoylmethanoate; phen= phenanthroline; hq= 8-hydroxy quinoline; Pc= phthalocyanine; TBA =N(C$_4$H$_9$)$_4$. H$_3$ATSA = 5-azotriazolyl salicylic acid.
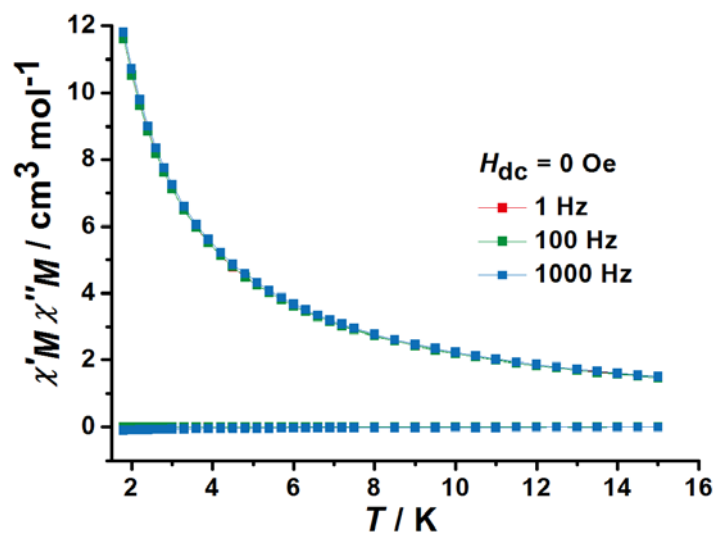
Fig. S10 Temperature dependence of the in-phase ($\chi_M'$) and out-of-phase ($\chi_M''$) products at zero dc field for **2**.
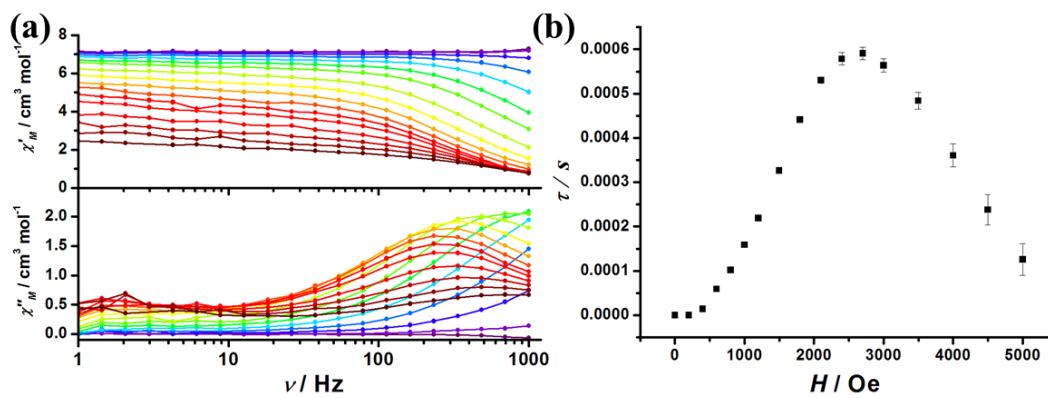


Fig. S11 (a) Frequency dependence of $\chi'_M$ and $\chi''_M$ signals at various fields at 3 K for **2**. The solid lines are guides to the eyes. (b) Field dependence of the magnetic relaxation time ($\tau$).

Table S5 Relaxation fitting parameters from Least-Squares Fitting of $\chi(\omega)$ data for **2** at various dc field at 3 K.

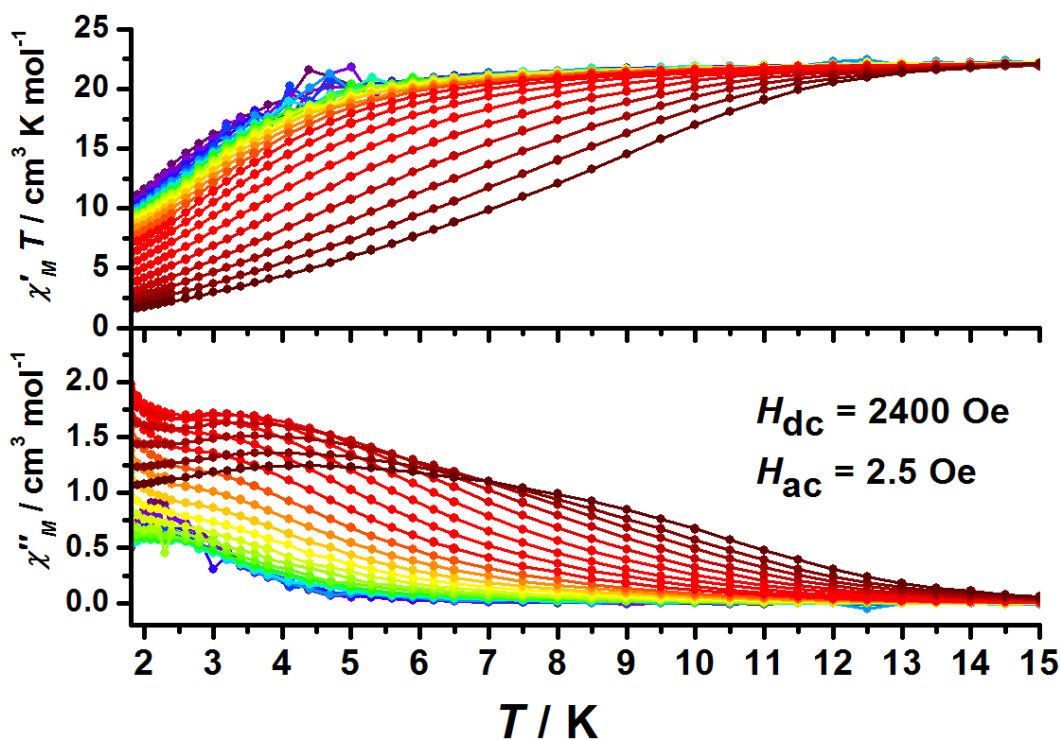| H / Oe | $\tau$ Value | $\tau$ Standard Error | $\alpha$ Value | $\alpha$ Standard Error | $\chi_0$ Value | $\chi_0$ Standard Error | $\chi_\infty$ Value | $\chi_\infty$ Standard Error |
|---|---|---|---|---|---|---|---|---|
| 0 | 2.13E-04 | 1.63E-05 | -0.53026 | 0.10216 | 7.14695 | 0.00533 | 7.21519 | 0.01452 |
| 200 | 7.93E-08 | 1.29E-04 | -0.21448 | 0.09941 | 7.10403 | 0.00533 | -1707.17 | 3.38E+06 |
| 400 | 1.42E-05 | 3.50E-06 | 0.11251 | 0.01233 | 7.03171 | 0.00331 | 0.16157 | 1.27277 |
| 600 | 5.90E-05 | 2.61E-06 | 0.10713 | 0.00664 | 6.90858 | 0.00404 | 2.24768 | 0.13773 |
| 800 | 1.02E-04 | 2.75E-06 | 0.12759 | 0.00591 | 6.75023 | 0.00606 | 1.71236 | 0.08556 |
| 1000 | 1.59E-04 | 3.13E-06 | 0.14982 | 0.00563 | 6.56926 | 0.00829 | 1.29197 | 0.06305 |
| 1200 | 2.19E-04 | 3.44E-06 | 0.17515 | 0.0052 | 6.36851 | 0.00984 | 0.87024 | 0.05024 |
| 1500 | 3.26E-04 | 4.44E-06 | 0.19401 | 0.0054 | 6.01044 | 0.01288 | 0.50013 | 0.04251 |
| 1800 | 4.41E-04 | 5.24E-06 | 0.20267 | 0.00536 | 5.63548 | 0.01435 | 0.3324 | 0.03503 |
| 2100 | 5.31E-04 | 6.68E-06 | 0.20748 | 0.00607 | 5.22548 | 0.01681 | 0.22011 | 0.03441 |
| 2400 | 5.79E-04 | 1.41E-05 | 0.2127 | 0.01201 | 4.79346 | 0.0324 | 0.12574 | 0.06121 |
| 2700 | 5.91E-04 | 1.43E-05 | 0.21946 | 0.01191 | 4.38855 | 0.03021 | 0.05728 | 0.05604 |
| 3000 | 5.64E-04 | 1.51E-05 | 0.2488 | 0.01222 | 4.05476 | 0.02925 | -0.04339 | 0.0568 |
| 3500 | 4.84E-04 | 1.91E-05 | 0.28979 | 0.01547 | 3.51625 | 0.03199 | -0.16205 | 0.07162 |
| 4000 | 3.61E-04 | 2.62E-05 | 0.35806 | 0.02096 | 3.0725 | 0.03818 | -0.37637 | 0.11052 |
| 4500 | 2.38E-04 | 3.45E-05 | 0.42758 | 0.028 | 2.68458 | 0.04521 | -0.62558 | 0.18182 |
| 5000 | 1.26E-04 | 3.57E-05 | 0.49986 | 0.03312 | 2.36578 | 0.04852 | -0.98853 | 0.30281 |



Fig. S12 Temperature dependence of the in-phase ($\chi_M'T$) and out-of-phase ($\chi_M''$) products at 2400 Oe field for **2**, with ac frequencies of 1−1000 Hz. The solid lines are guides to the eyes.

Table S6 Relaxation fitting parameters from Least-Squares Fitting of $\chi(\omega)$ data for 2 at 2400 Oe field.

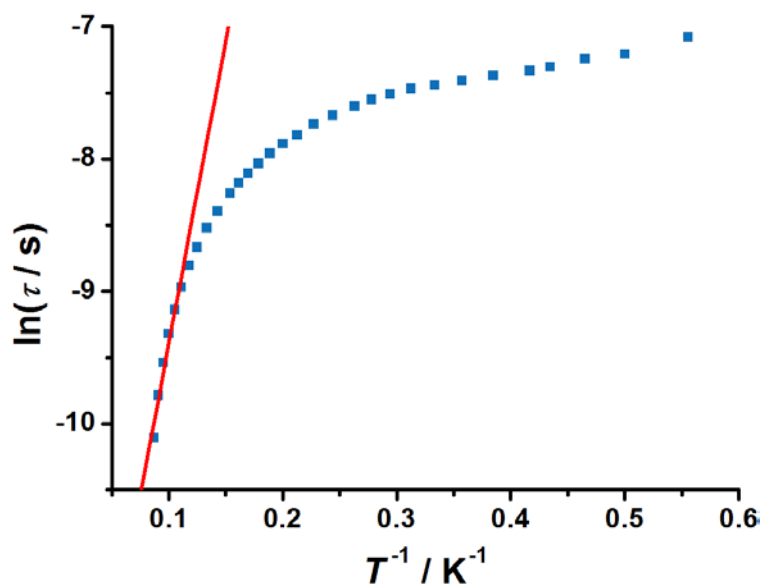| $T$ / K | $\tau$ | $\tau$ | $\alpha$ | $\alpha$ | $\chi_0$ | $\chi_0$ | $\chi_\infty$ | $\chi_\infty$ |
|---|---|---|---|---|---|---|---|---|
| | Value | Standard Error | Value | Standard Error | Value | Standard Error | Value | Standard Error |
| 1.8 | 8.42E-04 | 1.05E-05 | 0.18035 | 0.00684 | 5.4445 | 0.02224 | 0.24171 | 0.03362 |
| 1.9 | 7.87E-04 | 1.16E-05 | 0.19663 | 0.00778 | 5.26115 | 0.02408 | 0.19976 | 0.0387 |
| 2 | 7.42E-04 | 1.43E-05 | 0.20253 | 0.00993 | 5.12059 | 0.02938 | 0.17704 | 0.04972 |
| 2.15 | 7.14E-04 | 1.52E-05 | 0.21313 | 0.01067 | 5.06692 | 0.03109 | 0.14284 | 0.05453 |
| 2.3 | 6.73E-04 | 1.49E-05 | 0.21695 | 0.01079 | 4.96634 | 0.03013 | 0.1335 | 0.0557 |
| 2.4 | 6.53E-04 | 1.57E-05 | 0.22979 | 0.01133 | 4.95723 | 0.0317 | 0.08745 | 0.06032 |
| 2.6 | 6.30E-04 | 1.38E-05 | 0.23137 | 0.01021 | 4.94579 | 0.0281 | 0.08173 | 0.05524 |
| 2.8 | 6.07E-04 | 1.25E-05 | 0.22278 | 0.0096 | 4.92403 | 0.02565 | 0.0985 | 0.05203 |
| 3 | 5.85E-04 | 1.57E-05 | 0.21492 | 0.01259 | 4.89437 | 0.03264 | 0.1113 | 0.06841 |
| 3.2 | 5.70E-04 | 8.54E-06 | 0.20053 | 0.00715 | 4.85628 | 0.01783 | 0.16408 | 0.03816 |
| 3.4 | 5.47E-04 | 7.51E-06 | 0.18983 | 0.0066 | 4.7895 | 0.01575 | 0.19145 | 0.03491 |
| 3.6 | 5.26E-04 | 6.26E-06 | 0.18483 | 0.0057 | 4.72739 | 0.01309 | 0.20839 | 0.03005 |
| 3.8 | 4.99E-04 | 6.50E-06 | 0.17321 | 0.00626 | 4.61443 | 0.01355 | 0.23358 | 0.03253 |
| 4.1 | 4.66E-04 | 7.39E-06 | 0.1589 | 0.00764 | 4.45632 | 0.01524 | 0.27151 | 0.03884 |
| 4.4 | 4.36E-04 | 6.36E-06 | 0.14536 | 0.00704 | 4.30407 | 0.01292 | 0.31444 | 0.03493 |
| 4.7 | 4.02E-04 | 7.43E-06 | 0.13329 | 0.00885 | 4.11721 | 0.01477 | 0.33492 | 0.04304 |
| 5 | 3.77E-04 | 4.76E-06 | 0.12562 | 0.00599 | 3.97539 | 0.00922 | 0.36535 | 0.02857 |
| 5.3 | 3.50E-04 | 4.49E-06 | 0.12291 | 0.00591 | 3.82893 | 0.00839 | 0.37519 | 0.02798 |
| 5.6 | 3.25E-04 | 3.62E-06 | 0.11356 | 0.00506 | 3.66374 | 0.00652 | 0.39731 | 0.02342 |
| 5.9 | 3.01E-04 | 3.58E-06 | 0.10862 | 0.00525 | 3.51396 | 0.00618 | 0.40771 | 0.02404 |
| 6.2 | 2.80E-04 | 3.52E-06 | 0.10453 | 0.00539 | 3.37558 | 0.00579 | 0.42202 | 0.02439 |
| 6.5 | 2.59E-04 | 3.43E-06 | 0.10098 | 0.00548 | 3.24155 | 0.00537 | 0.43019 | 0.02459 |
| 7 | 2.26E-04 | 3.37E-06 | 0.09847 | 0.00573 | 3.03984 | 0.00482 | 0.42801 | 0.02587 |
| 7.5 | 1.99E-04 | 3.33E-06 | 0.0925 | 0.00601 | 2.8546 | 0.0043 | 0.44712 | 0.02704 |
| 8 | 1.72E-04 | 2.92E-06 | 0.09317 | 0.00552 | 2.6925 | 0.00337 | 0.43766 | 0.02558 |
| 8.5 | 1.50E-04 | 3.05E-06 | 0.08902 | 0.00607 | 2.54465 | 0.00313 | 0.45425 | 0.02863 |
| 9 | 1.27E-04 | 2.85E-06 | 0.08925 | 0.00594 | 2.41131 | 0.00256 | 0.45049 | 0.02952 |
| 9.5 | 1.07E-04 | 2.67E-06 | 0.08728 | 0.00584 | 2.29006 | 0.00208 | 0.45407 | 0.03089 |
| 10 | 8.96E-05 | 2.96E-06 | 0.08645 | 0.00676 | 2.18129 | 0.00195 | 0.46364 | 0.03854 |
| 10.5 | 7.20E-05 | 3.02E-06 | 0.09055 | 0.00722 | 2.08315 | 0.00167 | 0.45154 | 0.04659 |
| 11 | 5.63E-05 | 3.49E-06 | 0.09789 | 0.00879 | 1.99411 | 0.00161 | 0.42403 | 0.06661 |
| 11.5 | 4.08E-05 | 3.37E-06 | 0.10943 | 0.00907 | 1.91149 | 0.0013 | 0.33733 | 0.08937 |

Fig. S13 The plots of $\ln(\tau)$ vs. $T^{-1}$ for **2** under 2400 Oe dc fields. The red line represents fit the data in the high temperature region with an Arrhenius law, resulting in an energy barrier $U_{eff}$ = 32 (3) K, pre-exponential factor $\tau_0 = 8.4 \times 10^{-7}$ s.

# Computational details

Mononuclear complex **1** has two different structures indicated as **Dy1** and **Dy2** (see Fig. S14). Likewise, complex **2** also has two different structures indicated as **Tb1** and **Tb2**. Thus, the **Dy1** and **Dy2** for **1** and the **Tb1** and **Tb2** for **2** were calculated, respectively. Complete-active-space self-consistent field (CASSCF) calculations on the complete structures of **Dy1**, **Dy2**, **Tb1** and **Tb2** extracted from the compounds on the basis of single-crystal X-ray determined geometry have been carried out with MOLCAS 8.2[7-9] program package.

The basis sets for all atoms are atomic natural orbitals from the MOLCAS ANO-RCC library: ANO-RCC-VTZP for $Dy^{III}$ or $Tb^{III}$ ion; VTZ for close O; VDZ for distant atoms. The calculations employed the second order Douglas-Kroll-Hess Hamiltonian, where scalar relativistic contractions were taken into account in the basis set and the spin-orbit couplings were handled separately in the restricted active space state interaction (RASSI-SO) procedure. Active electrons in 7 active spaces include all $f$ electrons (CAS(9 in 7) for **Dy1** and **Dy2**, and CAS(8 in 7) for **Tb1** and **Tb2**) in the CASSCF calculation. To exclude all the doubts, we calculated all the roots in the active space. We have mixed the maximum number of spin-free state which was possible with our hardware (all from 21 sextets, 128 from 224 quadruplets, 130 from 490 doublets for **Dy1** and **Dy2**; all from 7 septets, all from 140 quintets and 68

from 500 triplets for **Tb1** and **Tb2**). Single−Aniso[10-12] program was used to obtain energy levels, **g**

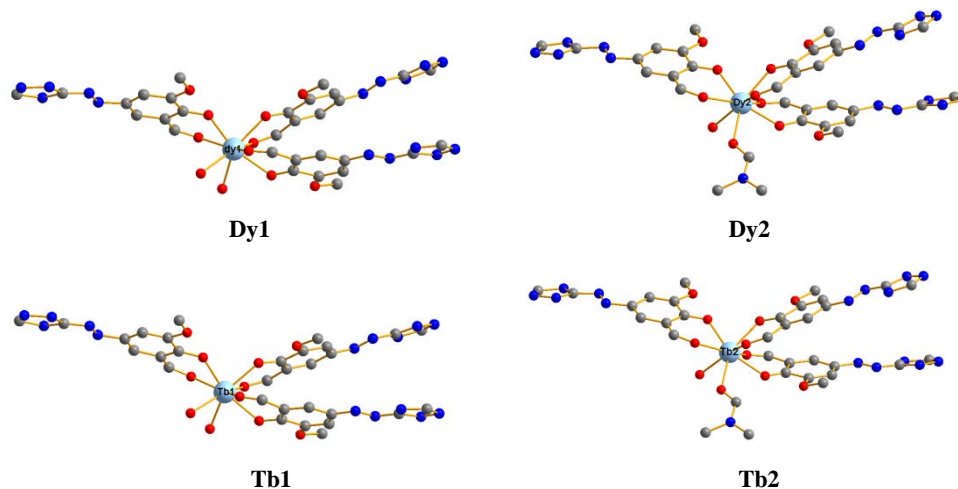tensors, $m_J$ values, magnetic axes, *et al.,* based on the above CASSCF/RASSI calculations.



**Fig. S14.** Calculated structures of **Dy1**, **Dy2**, **Tb1** and **Tb2**; H atoms are omitted.

**Table S7.** Calculated energy levels (cm$^{-1}$), **g** ($g_x$, $g_y$, $g_z$) tensors and $m_J$ values of the lowest eight or seven spin-orbit states of **Dy1**, **Dy2**, **Tb1** and **Tb2** using CASSCF/RASSI with MOLCAS 8.2.

|  | Dy1 | | | Dy2 | | |
|---|---|---|---|---|---|---|
|  | $E$/cm$^{-1}$ | **g** | $m_J$ | $E$/cm$^{-1}$ | **g** | $m_J$ |
| 1 | 0.0 | 0.003 0.004 19.700 | ±15/2 | 0.0 | 0.001 0.001 19.619 | ±15/2 |
| 2 | 169.3 | 0.038 0.078 16.975 | ±13/2 | 174.4 | 0.037 0.041 16.762 | ±13/2 |
| 3 | 248.3 | 2.549 3.151 15.487 | ±1/2 | 301.4 | 0.815 1.355 12.941 | ±11/2 |
| 4 | 281.8 | 9.072 6.510 0.275 | ±9/2 | 348.0 | 1.714 4.130 13.517 | ±7/2 |
| 5 | 342.0 | 2.902 4.681 10.056 | ±5/2 | 388.2 | 7.898 6.426 1.573 | ±5/2 |
| 6 | 364.7 | 0.754 2.169 16.691 | ±7/2 | 415.4 | 1.514 3.637 13.217 | ±3/2 |
| 7 | 421.8 | 0.174 0.251 17.565 | ±3/2 | 477.7 | 0.314 0.656 18.631 | ±1/2 |
| 8 | 535.2 | 0.003 0.019 | ±11/2 | 611.5 | 0.010 0.015 | ±9/2 |

| | | Tb1 | | | Tb2 | |
|---|---|---|---|---|---|---|
| | | 18.959 | | | 19.637 | |
| | | | | | | |
| | | **Tb1** | | | **Tb2** | |
| | $E$/cm$^{-1}$ | *g* | $m_J$ | $E$/cm$^{-1}$ | *g* | $m_J$ |
| 1 | 0.0 | 0.000 | ±6 | 0.0 | 0.000 | ±6 |
| | 0.07 | 0.000 | | 0.13 | 0.000 | |
| | | 17.769 | | | 17.626 | |
| 2 | 161.8 | 0.000 | ±5 | 102.9 | 0.000 | ±5 |
| | 162.1 | 0.000 | | 103.6 | 0.000 | |
| | | 14.778 | | | 15.607 | |
| 3 | 210.9 | 0.000 | ±3 | 148.6 | 0.000 | ±4 |
| | 212.7 | 0.000 | | 153.3 | 0.000 | |
| | | 15.494 | | | 11.990 | |
| 4 | 293.1 | 0.000 | ±4 | 224.9 | 0.000 | ±3 |
| | 301.3 | 0.000 | | 253.3 | 0.000 | |
| | | 9.377 | | | 8.202 | |
| 5 | 371.3 | 0.000 | ±1 | 290.5 | | 0 |
| | 390.4 | 0.000 | | | | |
| | | 5.787 | | | | |
| 6 | 422.5 | | 0 | 362.9 | 0.000 | ±1 |
| | | | | 372.6 | 0.000 | |
| | | | | | 13.425 | |
| 7 | 521.2 | 0.000 | ±2 | 532.8 | 0.000 | ±2 |
| | 525.1 | 0.000 | | 534.0 | 0.000 | |
| | | 16.662 | | | 17.078 | |

**Table S8.** Wave functions with definite projection of the total moment | $m_J$ > for the lowest two Kramers doublets (KDs) of **Dy1**, **Dy2**, **Tb1** and **Tb2** using CASSCF/RASSI with MOLCAS 8.2.

| | $E$/cm$^{-1}$ | wave functions |
|---|---|---|
| **Dy1** | 0.0 | 97%\|±15/2> |
| | 169.3 | 80%\|±13/2>+10%\|±11/2> |
| **Dy2** | 0.0 | 96%\|±15/2> |
| | 174.4 | 89%\|±13/2> |
| **Tb1** | 0.00 | 98%\|±6> |
| | 0.07 | |
| | 161.8 | 88%\|±5>+10%\|±3> |
| | 162.1 | |
| **Tb2** | 0.00 | 96%\|±6> |
| | 0.13 | |
| | 102.9 | 28%\|±6>+31%\|±5>+17%\|±3>+10%\|±2> |
| | 103.6 | |

To fit the exchange interactions between **Dy1** and **Dy2** in **1** (**Tb1** and **Tb2** in **2**), we took two steps to obtain them. Firstly, we calculated **Dy1**, **Dy2**, **Tb1** and **Tb2** using CASSCF to obtain the corresponding magnetic properties. Then, the exchange interaction between the magnetic centers is considered within the Lines model,[13] while the account of the dipole-dipole magnetic coupling is treated exactly. The Lines model is effective and has been successfully used widely in the research field of *f*-element single-molecule magnets.[14, 15]

For **1** and **2**, there is only one type of *J*.

The exchange Ising Hamiltonian are:

$$\boldsymbol{H}_{exch} = -J\boldsymbol{S}_{Dy1}\boldsymbol{S}_{Dy2} \tag{S1}$$

$$\boldsymbol{H}_{exch} = -J\boldsymbol{S}_{Tb1}\boldsymbol{S}_{Tb2} \tag{S2}$$

The *J* is the parameter of the total magnetic interaction ($J_{total} = J_{diploar} + J_{exchange}$) between magnetic center ions. The $\boldsymbol{S}_{Dy} = \pm 1/2$ and $\boldsymbol{S}_{Tb} = \pm 1/2$ are the ground pseudospin on $Dy^{III}$ and $Tb^{III}$ sites. The dipolar magnetic coupling can be calculated exactly, while the exchange coupling constants were fitted through comparison of the computed and measured magnetic susceptibilities using the Poly_Aniso program. [10-12]

**Table S9.** Exchange energies ($cm^{-1}$) and main values of the $g_z$ for the lowest two exchange doublets of **1** and **2**.

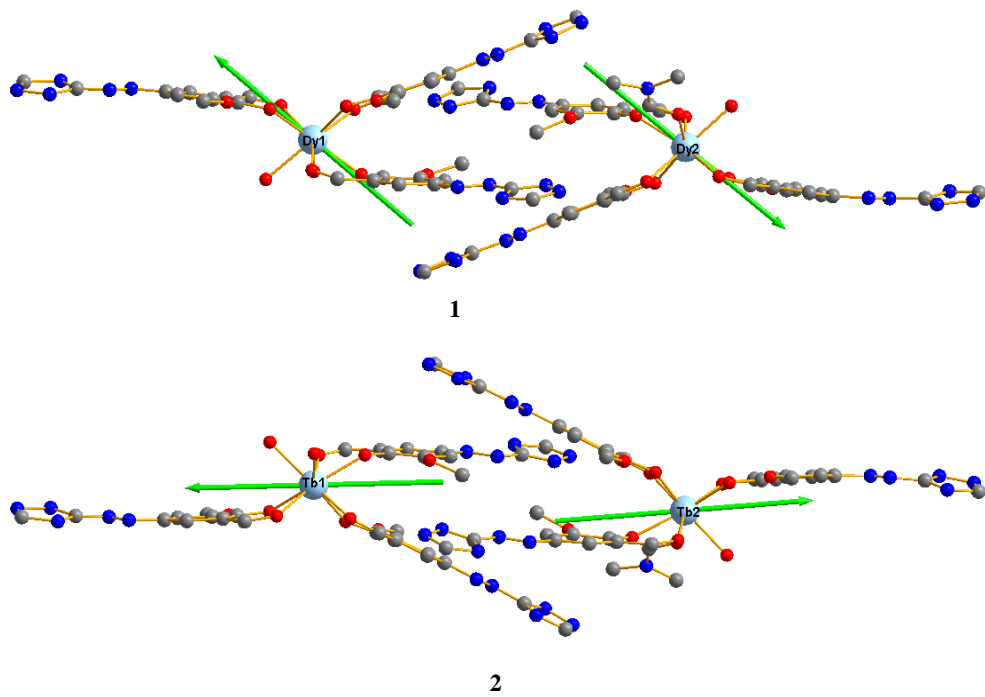|  | 1 | | 2 | |
|---|---|---|---|---|
|  | $E/cm^{-1}$ | $g_z$ | $E/cm^{-1}$ | $g_z$ |
| 1 | 0.0 | 2.802 | 0.0 | 4.115 |
| 2 | 0.1 | 39.219 | 0.2 | 30.207 |

**1**



**2**

**Fig. S15.** Calculated orientations of the local main magnetic axes in the ground spin-orbit state on Dy$^{III}$ ions of **1** and Tb$^{III}$ ions of **2**.

# References

1.      L.-F. Wang, J.-Z. Qiu, J.-Y. Hong, Y.-C. Chen, Q.-W. Li, J.-H. Jia, J. Jover, E. Ruiz, J.-L. Liu and M.-L. Tong, *Inorg. Chem.*, 2017, **56**, 8829-8836.

2.      S.-S. Liu, K. Lang, Y. Zhang, Q. Yang, B.-W. Wang and S. Gao, *Dalton Trans.*, 2016, DOI: 10.1039/C6DT01089J.

3.      S. D. Jiang, B. W. Wang, G. Su, Z. M. Wang and S. Gao, *Angew. Chem.Inter. Ed.*, 2010, **49**, 7448-7451.

4.      E. Moreno Pineda, N. F. Chilton, R. Marx, M. Dörfel, D. O. Sells, P. Neugebauer, S.-D. Jiang, D. Collison, J. van Slageren, E. J. L. McInnes and R. E. P. Winpenny, *Nat. Commun.*, 2014, **5**, 5243.

5.      N. Ishikawa, M. Sugita, T. Ishikawa, S.-y. Koshihara and Y. Kaizu, *J. Am. Chem. Soc.*, 2003, **125**, 8694-8695.

6.      L.-Q. Huang, Y.-Y. Lin, J.-D. Leng, J. Wang, L.-F. Yang and W. Dong, *Inorg. Chim. Acta*, 2018, **469**, 38-43.

7.      F. Aquilante, L. De Vico, N. Ferré, G. Ghigo, P.-å. Malmqvist, P. Neogrády, T. B. Pedersen, M. Pitoňák, M. Reiher, B. O. Roos, L. Serrano-Andrés, M. Urban, V. Veryazov and R. Lindh, *J. Comput. Chem.*, 2010, **31**, 224-247.

8.      V. Veryazov, P.-O. Widmark, L. Serrano-Andrés, R. Lindh and B. O. Roos, *Int. J. Quantum Chem*, 2004, **100**, 626-635.

9.      G. Karlström, R. Lindh, P.-Å. Malmqvist, B. O. Roos, U. Ryde, V. Veryazov, P.-O. Widmark, M. Cossi, B. Schimmelpfennig, P. Neogrady and L. Seijo, *Comput. Mater. Sci.*, 2003, **28**, 222-239.

10.     L. F. Chibotaru, L. Ungur and A. Soncini, *Angew. Chem. Int. Ed.*, 2008, **47**, 4126-4129.

11.     L. Ungur, W. Van den Heuvel and L. F. Chibotaru, *New J. Chem.*, 2009, **33**, 1224-1230.

12.     L. F. Chibotaru, L. Ungur, C. Aronica, H. Elmoll, G. Pilet and D. Luneau, *J. Am. Chem. Soc.*, 2008, **130**, 12445-12455.

13.     M. E. Lines, *The Journal of Chemical Physics*, 1971, **55**, 2977-2984.

14.     K. C. Mondal, A. Sundt, Y. Lan, G. E. Kostakis, O. Waldmann, L. Ungur, L. F. Chibotaru, C. E. Anson and A. K. Powell, *Angew. Chem. Int. Ed.*, 2012, **51**, 7550-7554.

15.     S. K. Langley, D. P. Wielechowski, V. Vieru, N. F. Chilton, B. Moubaraki, B. F. Abrahams, L. F. Chibotaru and K. S. Murray, *Angew. Chem. Int. Ed.*, 2013, **52**, 12014-12019.